scientific reports

Check for updates

OPEN

The SRG rat as a novel host for an orthotopic patient-derived xenograft model of breast cancer brain metastasis

Niveen Fulcher[1], Hien Nguyen[1], Andrew Deweyert[2], Mila Uzelac[2], Maryam Mozaffari[3], Qi Zhang[4], John A. Ronald[3], John J. Kelly[3], Ying Xia[3], Timothy J. Scholl[3,5], Fallon K. Noto[6], Diane Begemann[6], Michael J. Schlosser[6], Susanne Schmid[2] & Matthew O. Hebb[1]✉

Patient-derived xenograft (PDX) models are essential for understanding the pathophysiology and developing treatment strategies for breast cancer brain metastasis (BCBM). While immunodeficient mouse models allow for human BCBM growth, their small size limits host survival, neurological imaging and therapeutic interventions. This study evaluated the immunodeficient SRG rat (Sprague Dawley *Rag2−/−; Il2rg−/−*) as a new intermediate-sized host for orthotopic modeling of human BCBM. The primary goal was to determine if the SRG rat brain presents a hospitable environment for orthotopic growth of patient BCBM cells. A secondary goal was to compare phenotypes of the patient and xenografted tumors. Adult SRG rats received stereotactic intracerebral implants of 1 million engineered patient BCBM cells. Bioluminesence imaging (BLI) and magnetic resonance imaging (MRI) provided metabolic and anatomic monitoring of tumor growth. Post-mortem histological analysis compared biomarker profiles in original patient and xenograft tumors. Orthotopic patient-derived BCBM tumors progressed in all SRG rats within 5 weeks post-implantation. BLI radiance increased 125-fold over the study period. MRI revealed tumor-induced brain edema and both patient and xenograft BCBMs exhibited pronounced vascularity and gadolinium enhancement. Histopathology confirmed that xenograft tumors maintained high proliferation indices and biomarker expression consistent with the parent tumor. The SRG rat provided a reliable intermediate-sized host for orthotopic growth of patient-derived BCBM xenografts, offering advantages over existing models for studying tumor behavior and therapeutic responses.

Breast cancer is the most prevalent cancer and a leading cause of central nervous system (CNS) metastasis and cancer-related mortality among women[1]. The overall risk of developing breast cancer brain metastasis (BCBM) is estimated at 10–16%, increasing significantly to 25–40% for human epidermal growth factor receptor 2 (HER2+) subtypes and up to 46% for triple-negative breast cancer[2]. Unfortunately, median survival following BCBM diagnosis remains low, ranging from 6 to 27 months[2]. Current treatment options include surgery, radiotherapy and targeted chemotherapy, with recent advances in pharmacotherapeutics offering improved control of somatic disease[3]. Despite this progress, the limited ability of many systemically administered chemotherapies to cross the blood–brain barrier continues to reduce treatment efficacy in patients with BCBM[4].

To deepen our understanding of BCBM pathophysiology and tumor-brain interactions, effective research models are crucial for identifying cancer vulnerabilities that could inform new treatments. Experimental tumor platforms typically utilize animal or human-derived cancer cells or tissues in in vitro, ex vivo, or in vivo settings. While traditional 2D cell cultures and organotypic models facilitate high throughput and controlled studies, they fail to accurately emulate the native tumor microenvironment (TME) which can significantly influence cancer cell behavior and treatment responses[5]. There is a pressing need for more robust experimental platforms

[1]Department of Clinical Neurological Sciences, Schulich School of Medicine and Dentistry, University of Western Ontario, London, ON N6A 5A5, Canada. [2]Department of Anatomy and Cell Biology, Schulich School of Medicine and Dentistry, University of Western Ontario, London, ON, Canada. [3]Department of Medical Biophysics, Schulich School of Medicine and Dentistry, University of Western Ontario, London, ON, Canada. [4]Department of Pathology and Laboratory Medicine, Schulich School of Medicine and Dentistry, University of Western Ontario, London, ON, Canada. [5]Ontario Institute for Cancer Research, Toronto, ON, Canada. [6]Hera Biolabs, Lexington, KY, USA. ✉email: mhebb@uwo.ca

that ensure reliable cancer modeling while incorporating tumor genotypes and TMEs that closely mimic human conditions. Orthotopic patient-derived xenograft (PDX) models, which enable the growth of human tumors within a living experimental host, are continuously evolving as vital resources for cancer research.

Mice genetically engineered to diminish innate and adaptive immune responses are commonly employed for PDX studies[6]. Various immunodeficient mouse strains have been utilized to create a conducive environment for orthotopically implanted human brain tumors, including BCBM. The established reliability, cost-effectiveness and ease of handling of these models contribute to their widespread use. However, the small size of the mouse brain and stature presents significant limitations for high-resolution CNS imaging, neurosurgical and other targeted therapeutic interventions, complex behavioral studies and host survival. Larger animal models, including porcine and canine platforms, can potentially overcome these challenges, although they require ongoing immunosuppressive therapy to prevent graft rejection and entail much higher costs and logistical complexities, including availability[7].

In this study, we evaluated a novel intermediate-sized PDX host platform utilizing the SRG rat (Sprague Dawley *Rag2*−/−; *Il2rg*−/−) developed by Hera BioLabs in a preclinical BCBM model[8]. The SRG rat, a double knockout model, is characterized by the depletion of B cells, T cells and NK cells, resulting in significant immunodeficiency. This model has shown promise in hosting various human somatic cancers and is anticipated to be effective for orthotopic integration of human brain cancers[8]. There are numerous potential advantages of using the SRG rat over traditional mouse models. For instance, rat brains are approximately five times larger, allowing for enhanced anatomical resolution using clinically applicable imaging modalities like magnetic resonance imaging (MRI) and computed tomography (CT). The larger brain also facilitates more extensive translational approaches, including tumor resection and device implantation. Furthermore, rats exhibit relatively longer survival times in the presence of growing brain tumors, making them well-suited for behavioral studies and with easier intravenous access for blood draws or drug delivery[9]. To validate the SRG rat as a model host for human BCBM growth, we conducted an orthotopic PDX study that measured longitudinal tumor growth in the brain combined with a detailed imaging and histological comparison between the original patient and xenografted rat tumors.

Materials and methods

Breast cancer brain metastasis (BCBM) patient and cell culture

This study was approved by the Human Research Ethics Board at Western University and carried out in accordance with the Tri-Council Policy for research involving human subjects. Informed consent for tumor tissue was obtained preoperatively. The BCBM diagnosis was confirmed by a clinical neuropathologist. The female BCBM donor patient had a history of metachronous bilateral breast cancer with systemic metastasis treated over 3 decades with mastectomies and various courses of tamoxifen, doxorubicin, cyclophosphamide, pertuzumab, trastuzumab and paclitaxel. MRI subsequently revealed a complex ~ 5 cm gadolinium-enhancing, cystic and solid tumor in the frontal lobe, producing mass effect and cerebral edema. The systemic disease burden was relatively stable at that time and surgical resection was offered for the newly diagnosed BCBM. Both the original breast cancer and the BCBM were found to be estrogen receptor (ER)- and progesterone receptor (PR)- negative, but HER2-positive. BCBM tissue was collected into phosphate-buffered saline (PBS) at the time of surgery and transferred directly to the lab. The tissue was mechanically digested, filtered then suspended in Dulbecco's modified Eagle's medium (DMEM; Wisent Bioproducts) supplemented with 10% FBS, 1% non-essential amino acids and 1% penicillin/streptomycin (Life Technologies). Tissue homogenates were plated on a 35 mm dish for 30 min to allow for separation of blood cells. The upper cell suspension was transferred to 24-well plates and incubated at 37 °C with 5% CO_2. Cultures were passaged at approximately 80% confluence and split 1:2 using 0.25% trypsin with 0.53 mM ethylenediaminetetraacetic acid (EDTA; Wisent). The medium was changed twice per week. Early passage cells (≤ 6) were transduced, as described, to express firefly luciferase (FLuc) and the tdTomato (tdT) reporter for bioluminescence imaging (BLI) and fluorescence histological localization, respectively[10].

Patient-derived xenografts in SRG rats

All animal protocols were approved by the Animal Care and Use Committee at Western University and carried out in accordance with the Tri-Council Policy for research involving human subjects and the Canadian Council on Animal Care. Adult male SRG male rats (N = 6; age 12–18 months; distributed by Charles River Laboratories for Hera BioLabs) were used due to their larger size, with an average weight of 363 g at the time of surgery. Rats were anesthetized with isoflurane (5% induction, 2% maintenance in 2L/min O_2) and positioned in a small animal stereotaxic frame. BCBM xenografts (10^6 cells in 10 µL PBS) were implanted via burrhole access into the caudate-putamen using coordinates from bregma: anteroposterior + 1.0 mm, lateral ± 3.0 mm, dorsoventral—6.5 mm. Cells were grafted into randomly chosen right or left hemispheres and delivered using a 10 µL Hamilton syringe. All rats received perioperative antibiotic (10 mg/kg enrofloxacin) and analgesic (1 mg/kg meloxicam). Study endpoint was determined through daily medical and neurological monitoring using institutional criteria (e.g., new neurological deficit, heightened pain, weight loss 15% or greater) for proceeding with euthanasia.

Tumor imaging

SRG rats were monitored longitudinally using BLI to assess tumor viability and growth. D-Luciferin (Syd Labs) was resuspended in Dulbecco's PBS (i.e., PBS without Mg^{2+} and Ca^{2+}) to a final concentration of 30 mg/mL. Rats were anesthetized followed by i.p. injection of 150 mg/kg of the luciferin substrate. Rats were then immediately placed in an In vivo Imaging System (IVIS) machine (Lumina XRMS Series III; PerkinElmer) and Living Image® software v.4.7.3 was used to measure the light signal emitted by luciferase-expressing cells. Exposure was set to 60 s and one image was taken every minute. BLI signal peak was determined when the signal decreased over two

consecutive images. BLI measures were initially taken within 10 days following BCBM cell implantation then weekly thereafter until rats reached a humane medical endpoint.

A representative SRG rat (SRG1) was assessed with gadolinium-enhanced cranial MRI on the terminal study day to validate BCBM tumor size, vascularity and imaging characteristics relative to the parent tumor. This was performed on a GE Discovery MR 750 3T MRI (General Electric Healthcare) using a custom-built 8-rung RF birdcage coil designed for rat head imaging. The rat was anesthetized with 2% isoflurane and positioned in a lab-built tray warmed to 38 °C. T1-weighted images were acquired 30 s after tail vein injection of gadolinium contrast agent (Magnevist, 0.5 mmol/kg, Bayer) using the following acquisition parameters: pulse sequence: 3D-FSE (fast spin echo); Echo Train Length (ETL) = 10; matrix size = 128 × 128 (Zero padded to 256 × 256); slice thickness = 0.5 cm; 112 slices; FOV = 6 cm; TR = 347 ms; TE = 18.672 ms; pixel bandwidth = 244.141 Hz; number of averages = 1; total acquisition time = 8.3 min. The rat brain MRI was compared to a clinical 3D-FSPGR (fast spoiled gradient echo) MRI with gadolinium administration obtained in the human patient prior to BCBM resection.

BCBM tissue analysis

The study termination date was guided for each rat by daily neurological and medical health monitoring. Signs of physical discomfort or decline in function or weight prompted a final BLI scan followed by pentobarbital or CO_2 euthanasia. SRG rat brains were promptly extracted and fixed with 10% formalin then cryoprotected and frozen (N = 2) or paraffin embedded (N = 4) for histological processing. The frozen brains were cut on a cryostat into 40 µm-thick sections through the rostrocaudal extent of the tumor. Sections were mounted onto microscope slides and cover-slipped with the mounting medium Fluoroshield™ with DAPI (Sigma-Aldrich) to define BCBM tumors expressing the tdTomato reporter against a DAPI-stained background. Processed sections were digitally imaged with a Nikon Eclipse Ni-E microscope at 10× magnification and the fluorochrome imaging merged using Zen software (Zeiss). The second subset of brains (N = 4) were processed in gradient ethanol, xylene, embedded in paraffin, sectioned into 4 µm-thick tissue slices and stained with Hematoxylin and Eosin (H&E). Immunohistochemical staining was performed using a Dako Omnis automatic stainer according to the user manual. All primary antibodies were prediluted ready-to-use mouse monoclonal antibodies from Dako, including CK-pan, CK7, CK20, mammaglobin, ER, PR and Ki67, except the HER2 A0480 antibody (1:800, rabbit polyclonal, Dako). Stained tissue sections were scanned using the Aperio XT automated scanning system (Leica Biosystems) and analyzed by a clinical neuropathologist (Q.Z.).

Data analyses

BLI peak values were recorded as average radiance (photons/second/cm^2/steradian). Selected regions of interest (ROIs) per animal remained the same to compare within-subjects across time. Rstudio was used to conduct a linear mixed-effects one-way analysis of variance (ANOVA) to evaluate the tumor growth levels of rats over 5 weeks with the Satterthwaite method. The employed R packages were Matrix and lme4 for fitting mixed-effects models, lmerTest for statistical tests within mixed models, reshape2 for data reshaping and ggplot2 for data visualization. Type III ANOVA followed by a Tukey post-hoc test and the Satterthwaite method were chosen to analyze how tumor growth varies across the 5 weeks while accounting for individual differences among rats by approximating the degrees of freedom in a fixed linear mixed-effects model. In addition, a paired, two-tailed Student t-test was conducted by GraphPad Prism (v9.0, (GraphPad Software) to compare the mean radiance from the cohort's first versus last BLI scan. All values are expressed as mean ± standard error of the mean (SEM).

The immunohistochemical analysis was performed by a clinical neuropathologist (Q.Z.). The Ki67 index was calculated using the web application, (http://www.ai4path.ca/#/ki67/si). HER2 was quantified as 0 (negative): no staining observed or incomplete faint / barely perceptible membrane staining within ≤ 10% of invasive tumor cells; 1 + (negative): incomplete faint membrane staining and within > 10% of invasive tumor cells; 2 + (equivocal): weak to moderate complete membrane staining observed in > 10% of invasive tumor cells; 3 + (positive): tumor displays complete, intense circumferential membranous staining in > 10% of tumor cells. Other IHC markers were semi-quantified using: + weak and focal; ++ moderate intensity, +++ diffuse and strong staining; by visual estimation of the stained sections.

Results

Orthotopic growth of human BCBM in the SRG rat brain

Stereotactic implantation of patient-derived BCBM cells consistently resulted in rapid tumor formation in the brains of six consecutive SRG rats. The growth and neurological impact of the PDX tumors were closely monitored through weekly BLI as well as daily medical and neurological evaluations. Notably, three of the rats survived until the fifth week, although they ultimately reached the medical endpoint due to complications arising from the BCBM. In contrast, two rats met this threshold in postoperative week 3, while one did so in week 4. The average duration of tumor growth following the BCBM cell implantation was 29 days, with individual durations ranging from 17 to 35 days across the cohort. Throughout the study period, rats experienced an average body weight loss of approximately 7% (equating to around 25 g), reflecting the physiological impact of tumor growth.

BLI analysis of the rat tumors revealed a dramatic increase in radiance intensity, with notable tumor expansion between the first and last BLI scan of each rat (Fig. 1A). The mean radiance of the entire cohort (N = 6) increased 125-fold over the study period, measured at 40,836 p/sec/cm^2/sr during initial BLI acquisition versus 5,096,167 p/sec/cm^2/sr at the terminal scan ($p = 0.001$, T-test, Fig. 1B). The individual peak BLI measures (p/sec/cm^2/sr) at endpoint were SRG1: 5.88E+6, SRG2: 3.32E+6, SRG3: 2.61E+6, SRG4: 7.98E+6, SRG5: 5.40E+6, SRG6: 5.39E+6. When week-to-week BLI measures were evaluated, there was a significant rise in radiance levels and thereby tumor growth, over the 5-week imaging period ($p = 0.007$; ANOVA). Posthoc analysis further showed a significant increase in mean radiance values in subsets of rats analyzed within 1 week of the BCBM implant

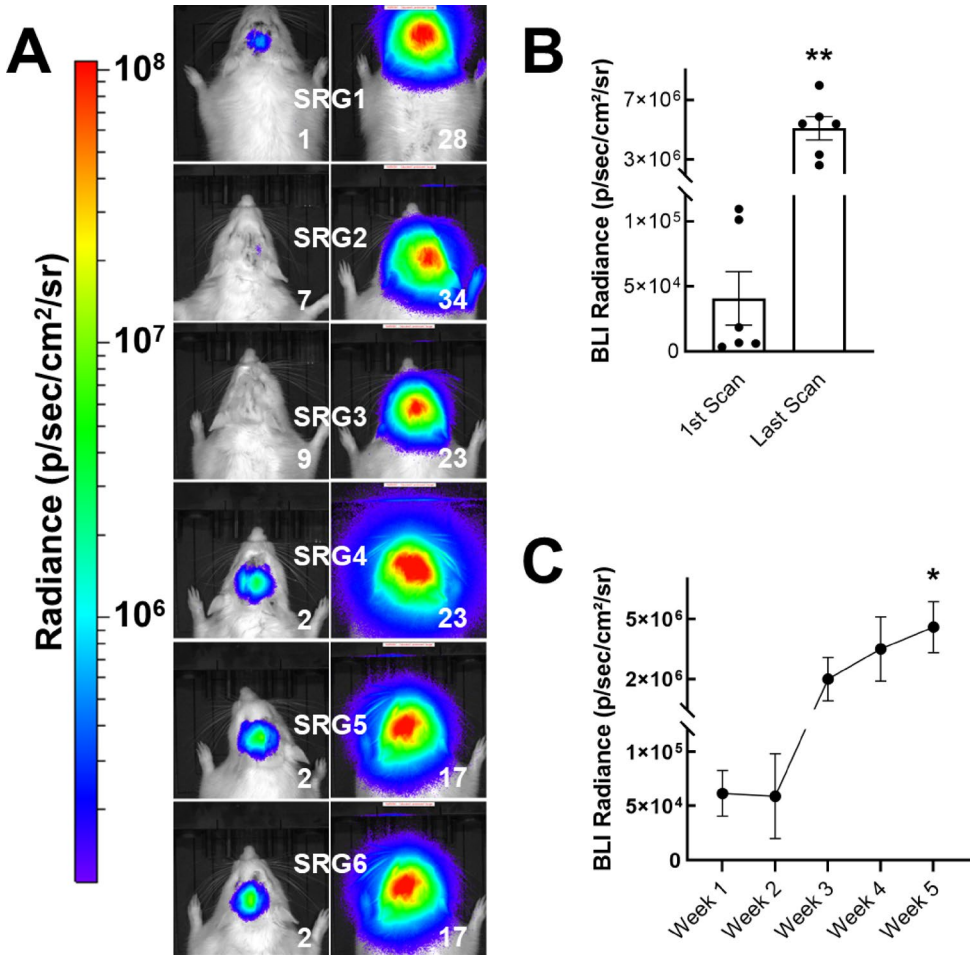

Fig. 1. Bioluminescence imaging (BLI) of orthotopic human BCBM growth in SRG rats. (**A**) BLI radiance levels (p/sec/cm^2/sr) shown for individual rats on different days post-transplant (post-implant day of imaging is indicated by white numbers in the lower-right corner of each image). The color scale bar on the left represents the intensity of radiance, increasing from low (blue) to high (red). (**B**) Quantification of BLI radiance levels comparing the first BLI scan to the last BLI scan in six rats. Individual values, as well as the mean ± standard errors are shown (**$p < 0.01$, T-test). (**C**) Mean BLI plotted over the course of 5 weeks shows significant increase in tumor radiance intensity ($p = 0.007$, ANOVA) and difference between week 1 and week 5 intensity (*$p < 0.05$; Tukey). Data are expressed as mean ± standard error.

(61,576 p/sec/cm^2/sr; N = 5) and those that received a BLI scan at week 5 (4,596,500 p/sec/cm^2/sr; $p = 0.039$; N = 2; Tukey, Fig. 1C).

A pre-operative brain MRI was performed on the human patient who served as the source of the tumor cells used in the SRG rat transplants (Fig. 2A,B). To compare the radiological character of the original human tumor to the PDX BCBM tumors, a representative rat underwent a brain MRI following the last BLI scan (SRG1, postoperative day 28, Fig. 2C,D). The MRI studies, which included intravenous administration of a gadolinium contrast agent, revealed similarities between the original human and the rat PDX tumors, as well as the surrounding brain parenchyma. Both tumor types presented as large, lobulated masses integrated within the brain tissue, with pronounced neovascularization and strong uptake of gadolinium. Additionally, there were signs of associated cerebral compression and vasogenic edema, consistent with similar pathological progression in both the human and rat brain. The fluorescence histological views of postmortem SRG rat brains revealed intense tdTomato reporter expression, consistent with tumor cell viability and the flourishing BCBM growth indicated by the BLI measures (Fig. 2E).

Histological comparison between original patient BCBM and PDX tumors

SRG rat brains were processed for clinicopathological analysis and compared directly with that of the original patient BCBM. The tumors were very large and many extended past the dorsal cortical surface. The disrupted anatomy proved challenging to precisely measure tumor dimensions, with a range of maximal diameter estimated between 4 and 6 mm (Fig. 3). H&E staining revealed tumor demarcation from the surrounding brain tissue in both patient and rat specimens. The patient BCBM consisted of moderately differentiated carcinoma

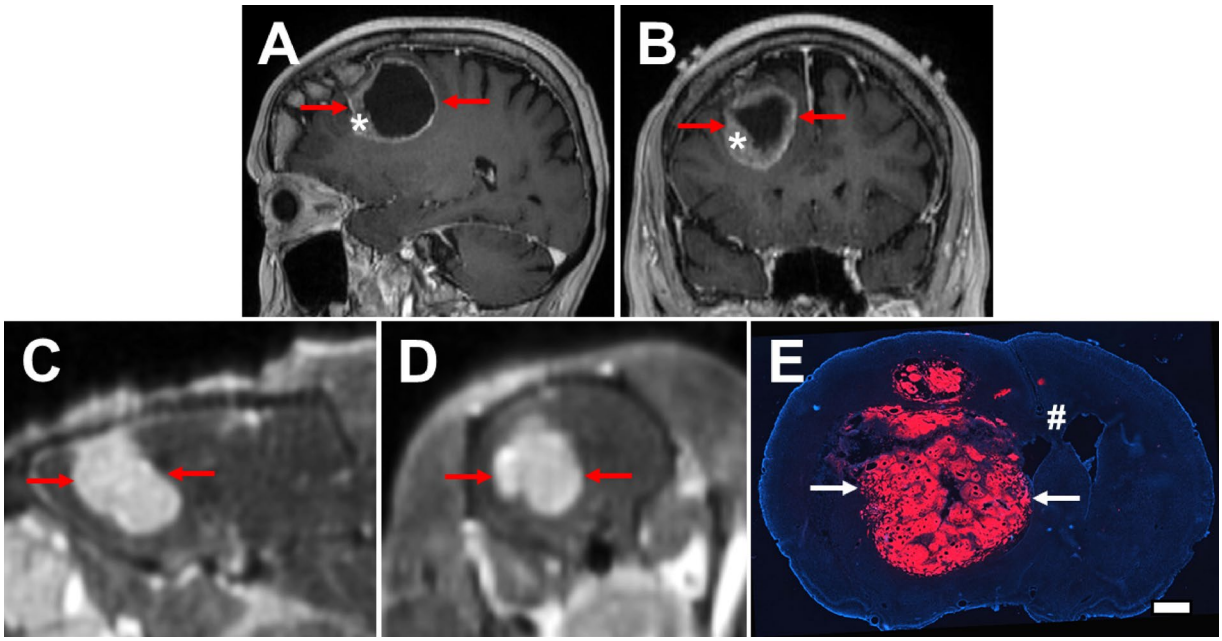

Fig. 2. Imaging features of patient and SRG rat BCBM tumors. T1-weighted MRI with gadolinium administration in (**A**,**B**) the donor human and (**C**,**D**) a representative SRG rat (SRG1). Sagittal (**A**,**C**) and coronal (**B**,**D**) views of the brain and BCBM tumors (arrows) are shown. The patient's BCBM was a large solid-cystic mass with gadolinium-enhancing tissue, producing regional cerebral edema and mass effect on the surrounding brain. The location of tissue collection for cell processing is marked with an asterisk. Likewise, the rat PDX tumor was avidly enhancing with gadolinium, and produced elevated intracranial pressure from cerebral edema and mass effect. (**E**) Histological brain section from the SRG1 rat (shown in **C** and **D**) viewed under fluorescence microscopy. The tdTomato reporter (red) in the PDX BCBM cells highlights the massive tumor (arrows) against a DAPI background-stained brain. The BCBM is demarcated from, yet integrated within, the brain tissue. The brain midline (#) is shifted contralaterally due to the large tumor. The scale bar in (**E**) estimates 1 mm.

with rudimentary glandular structures whereas the PDX tumor cells appeared poorly differentiated, forming sheets or nests of epithelioid cells without obvious glandular units (Fig. 3).

Immunohistochemical staining showed both similarities and distinctions between the human and PDX tumors. Pan cytokeratin (CK-pan) is an epithelium-specific antigen observed in most carcinomas and was strongly positive in the patient BCBM and the 5 PDX tumors evaluated. Breast carcinomas typically label negative for cytokeratin-20 (CK20) and positive for cytokeratin-7 (CK7), and this held true in the patient source BCBM, while the rat PDX tumors were negative for both markers[11]. Other markers used to characterize metastatic breast carcinoma include the estrogen (ER) and progesterone (PR) hormone receptors and mammaglobin[12]. The original patient BCBM in this study expressed intense levels of mammaglobin, but neither ER nor PR. The rat BCBM tumors also did not exhibit ER or PR labeling, nor was mammaglobin expression identified. The measured expression of human epidermal growth factor receptor-2 (HER2) is recommended upon primary breast cancer diagnosis, relapsed and metastatic settings to inform treatment decisions[13]. The original patient tumor was strongly positive, evaluated as 3+ using a conventional semi-quantitative clinicopathological scoring paradigm[14]. In the SRG rats, only 1 of 4 evaluated BCBM tumors showed strong, focal HER2 expression whereas the others had negligible labeling (Fig. 3).

The Ki67 proliferation index is a well-established prognostic factor in breast cancer, serving as an indicator of tumor cell proliferation[15]. In this study, the Ki67 index in the patient BCBM was calculated to be approximately 20%, consistent with active growth and previous reports indicating that a Ki67 index at this threshold is associated with more aggressive disease and poorer outcomes[16,17]. In comparison, the PDX tumors demonstrated significantly elevated Ki67 indices, exceeding 50% across all specimens sampled ($p < 0.01$; T-test; Fig. 3).

Discussion

Previous research established that SRG rats can effectively support somatic PDX cancers; however, the growth of human tumors within the living SRG rat brain has not been reported until now[6,8]. The primary objective of this study was to assess whether the SRG rat brain provides a hospitable environment for orthotopic growth of patient-derived BCBM tumors. A secondary aim was to compare the phenotype of the brain tumors from the original patient and the xenograft rat hosts. All SRG rats demonstrated robust development of human BCBM following tumor cell implantation in the brain. BLI enabled the longitudinal quantification of BCBM growth in vivo, while MRI showed robust brain integration and gadolinium enhancement, indicative of neovascularization and compromised integrity of the blood-tumor barrier, as seen in the original tumor pathology[18,19]. The PDX

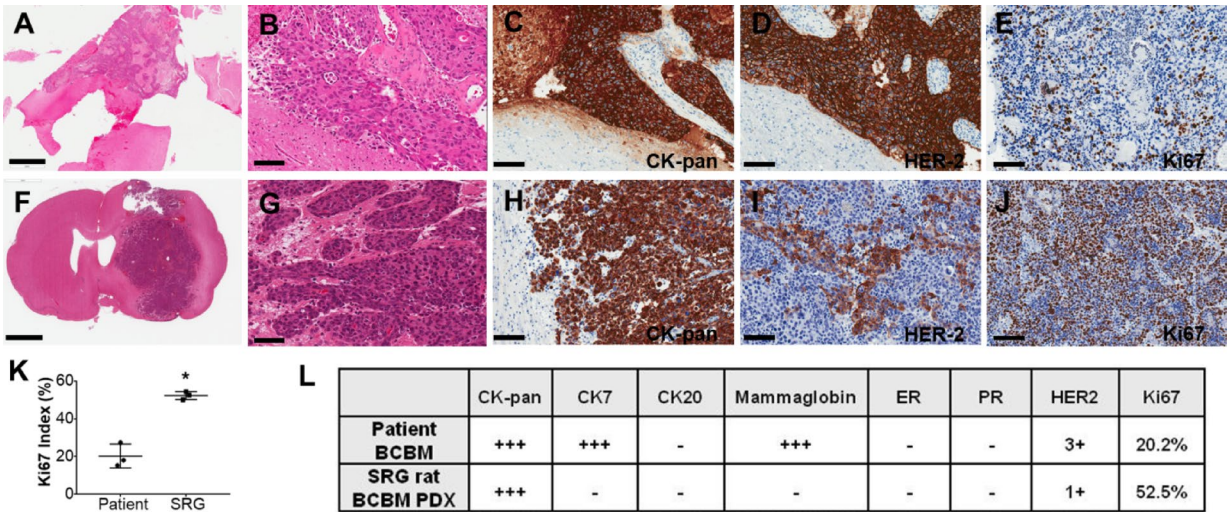

L

	CK-pan	CK7	CK20	Mammaglobin	ER	PR	HER2	Ki67
Patient BCBM	+++	+++	-	+++	-	-	3+	20.2%
SRG rat BCBM PDX	+++	-	-	-	-	-	1+	52.5%

Fig. 3. Histological comparison of the original patient and SRG rat PDX BCBM tumors. (**A**–**E**) The original patient BCBM histology and representative immunohistochemistry staining is shown. (**A**,**B**) H&E stain shows the breast metastasis is demarcated from brain tissue and composed of moderated differentiated carcinoma with poorly formed glandular structures. (**C**) It is strongly positive for pan-CK, (**D**) HER2 and (**E**) Ki67. (**F**,**G**) H&E stain of a representative SRG rat (SRG3) brain. The PDX BCBM tumors created from the patient BCBM cells are similarly demarcated from, but well integrated into, the rat brain. The PDX carcinoma cells are poorly differentiated, as sheets or nests of epithelioid cells without glandular formation. These cells are positive for (**H**) pan-CK, (**I**) HER2 (focal only, seen in 1 of 4 tumors) and (**J**) Ki67. (**K**) There is a significantly increased Ki67 index in the SRG tumors in comparison to the patient BCBM (*$p < 0.01$, T-Test). (**L**) The panel of immunohistochemistry markers are summarized. Scale bar in (**A**) and (**F**): 2 mm; in (**B**–**E**) and (**G**–**J**): 100 µm.

histology also confirmed maintenance of a mesenchymal phenotype and high proliferative index. The similarities between the patient and SRG rat BCBMs were offset by observed differences that merit consideration. For instance, the rat tumors exhibited loss of CK7 and mammaglobin expression, which were present in the original tumor, and decreased levels of HER2 expression. Additionally, detection of the Ki-67 mitotic indicator rose from 20% in the parent tumor to 52% in daughter BCBMs. These differences may reflect phenotype drift during tumor cell passage in vitro or within the new host, leading to genomic and physiological deviations from the original tumor. Luciferase was introduced into patient tumor cells using a lentiviral vector to enable BLI surveillance after implantation. Although there is a low probability that viral integration disrupted the expression of an unrelated gene, this remains a possibility. However, the chance that such disruption would involve a gene associated with BCBM—and even more so, multiple genes linked to key BCBM markers such as CK7, mammaglobin, and HER2—is exceedingly remote[20–23]. BLI was used as a surrogate for tumor growth and size and complements anatomic imaging with a metabolic measure of BCBM viability[10]. Given the tissue disruption and artifact with histological sectioning, and the notably irregular distribution of the intracerebral tumor, future work may consider MRI analysis to calculate tumor volume within the living rat brain. Male rats were used in this study primarily owing to the size advantage over female rats, and thereby sex-based hormonal discrepancies could also potentially influence BCBM cell phenotype[24,25]. Another contributing factor to the immunohistochemical profile of PDX tumors may relate to a predisposition of the parent BCBM cells to de-differentiate, a phenomenon linked to various cancer therapies that decreases expression of lineage-specific markers while increasing mitotic frequency[26,27]. The BCBM patient and tumor donor in this study had previously undergone radiation therapy and a range of pharmacological treatments throughout her cancer care, including tamoxifen, pertuzumab, trastuzumab and paclitaxel. Radiation therapy can select populations of de-differentiated breast cancer cells and induce stress responses that activate signaling pathways to promote a stem-like phenotype in surviving cells[28,29]. Tamoxifen primarily functions as an anti-estrogen therapy by blocking estrogen receptors and inhibiting tumor growth in hormone receptor-positive breast cancer. However, it can also activate pathways that encourage a more stem-like phenotype and potentially lead to de-differentiation[30,31]. Similar effects have also been observed with paclitaxel and HER2-targeted therapies such as pertuzumab and trastuzumab[32,33]. The data generated from this inaugural study will provide a springboard for future work focused on model refinement and determinants of the resultant PDX tumor phenotype.

There are benefits and limitations to consider when choosing a rat versus mouse model for brain cancer research.. The larger size of the rat brain allows for more extensive surgical manipulation and accommodation of larger tumors, longer survival time and study of complex tumor dynamics and animal behavior[9]. Clinical imaging modalities, such as CT and MRI, may also yield higher quality and resolution in the rat brain. Pharmacokinetics often differ between species, with rats offering more accurate predictions of human responses to certain agents which can be critical in the development of novel therapeutics[34–36]. Despite these advantages, mouse models have dominated in vivo cancer research due, in part, to the genetic manipulation potential and the wealth of historical data available for comparison[37,38]. Access to genetically engineered mouse platforms have enabled

targeting of specific oncogenic and cancer regulatory pathways but development of such engineered rat models is still in its infancy[39,40]. A critical feature of PDX platforms is their reliance on host animals with immunodeficient backgrounds. The SRG rat is particularly advantageous for xenografting due to its profound lack of functional T, B and NK cells, limiting the detrimental impact of a host immune response against foreign tissues[8,41]. This immunodeficiency is crucial for investigating the in vivo properties of human cancers but constrains the ability to understand the interactions between tumors and the immune system, an area that is gaining increasing significance in the development of cancer therapies. To address this limitation, the humanization of rat models, including the SRG model, has emerged as a promising approach. By incorporating human immune cells and elements of the human immune microenvironment, these advanced platforms may more accurately reflect the complexities of tumor-immune system interactions[41–43].

The limited availability of PDX brain cancer models in hosts larger than mice underscores the need to explore alternative platforms—such as rats—that may offer experimental advantages. The SRG rat represents a promising intermediate-sized host for PDX-based studies and a novel resource for investigating human BCBM. In this study, direct implantation of tumor cells into the brain was used to establish localized tumors. While this method does not replicate the full systemic process of metastasis, it is a well-established approach in other metastatic cancer models and provides a reliable means of generating brain tumors for preclinical evaluation of therapies, diagnostics and aspects of cancer pathophysiology[44,45]. Though it bypasses the natural metastatic cascade, orthotopic implantation can also serve as an important starting point for developing more advanced metastasis models. For example, demonstrating that tumor cells can successfully engraft and proliferate in the brain after direct injection suggests that systemic inoculation using the same biological components may hold promise for future applications. Ultimately, this orthotopic SRG rat platform provides a valuable proof of principle for studying BCBM and lays the groundwork for broader efforts to model both primary and metastatic human brain tumors.

Data availability

All data generated or analysed during this study are included in this published article.

Received: 28 November 2024; Accepted: 5 June 2025
Published online: 01 July 2025

References

1. Atkins, S. L. P. & Zimmer, A. S. Neurologic complications of breast cancer. *Cancer* **129**, 505–520. https://doi.org/10.1002/cncr.34518 (2023).
2. Raghavendra, A. S. & Ibrahim, N. K. Breast cancer brain metastasis: A comprehensive review. *JCO Oncol. Pract.* **20**, 1348–1359. https://doi.org/10.1200/OP.23.00794 (2024).
3. Liu, B. et al. Exploring treatment options in cancer: tumor treatment strategies. *Sig. Transduct. Target Ther.* **9**, 1–44. https://doi.org/10.1038/s41392-024-01856-7 (2024).
4. Arvanitis, C. D., Ferraro, G. B. & Jain, R. K. The blood–brain barrier and blood–tumour barrier in brain tumours and metastases. *Nat. Rev. Cancer* **20**, 26–41. https://doi.org/10.1038/s41568-019-0205-x (2020).
5. Yuki, K., Cheng, N., Nakano, M. & Kuo, C. J. Organoid Models of tumor immunology. *Trends Immunol.* **41**, 652–664. https://doi.org/10.1016/j.it.2020.06.010 (2020).
6. Liu, Y. et al. Patient-derived xenograft models in cancer therapy: technologies and applications. *Sig. Transduct. Target Ther.* **8**, 1–24. https://doi.org/10.1038/s41392-023-01419-2 (2023).
7. Ribitsch, I. et al. Large animal models in regenerative medicine and tissue engineering: To do or not to do. *Front. Bioeng. Biotechnol.* **8**, 972. https://doi.org/10.3389/fbioe.2020.00972 (2020).
8. Noto, F. K. et al. The SRG rat, a sprague-dawley Rag2/Il2rg double-knockout validated for human tumor oncology studies. *PLoS ONE* **15**, e0240169. https://doi.org/10.1371/journal.pone.0240169 (2020).
9. Sahu, U. et al. Rat and mouse brain tumor models for experimental neuro-oncology research. *J. Neuropathol. Exp. Neurol.* **81**, 312–329. https://doi.org/10.1093/jnen/nlac021 (2022).
10. Parkins, K. M. et al. A multimodality imaging model to track viable breast cancer cells from single arrest to metastasis in the mouse brain. *Sci. Rep.* **6**, 35889. https://doi.org/10.1038/srep35889 (2016).
11. Tot, T. Patterns of distribution of cytokeratins 20 and 7 in special types of invasive breast carcinoma: A study of 123 cases. *Ann. Diagn. Pathol.* **3**, 350–356. https://doi.org/10.1016/S1092-9134(99)80013-6 (1999).
12. Lopez-Gonzalez, L. et al. Exploring biomarkers in breast cancer: Hallmarks of diagnosis, treatment, and follow-up in clinical practice. *Medicina* **60**, 168. https://doi.org/10.3390/medicina60010168 (2024).
13. Yi, Z. et al. Molecular landscape and efficacy of HER2-targeted therapy in patients with HER2-mutated metastatic breast cancer. *npj Breast Cancer* **6**, 1–8. https://doi.org/10.1038/s41523-020-00201-9 (2020).
14. Palm, C. et al. Determining HER2 status by artificial intelligence: An investigation of primary, metastatic, and HER2 low breast tumors. *Diagnostics* **13**, 168. https://doi.org/10.3390/diagnostics13010168 (2023).
15. Yerushalmi, R. et al. Ki67 in breast cancer: prognostic and predictive potential. *Lancet Oncol.* **11**, 174–183. https://doi.org/10.1016/S1470-2045(09)70262-1 (2010).
16. Goldhirsch, A. et al. Personalizing the treatment of women with early breast cancer: Highlights of the St Gallen international expert consensus on the primary therapy of early breast cancer 2013. *Ann. Oncol.* **24**, 2206. https://doi.org/10.1093/annonc/mdt303 (2013).
17. Dowsett, M. et al. Assessment of Ki67 in breast cancer: Recommendations from the International Ki67 in Breast cancer working group. *JNCI J. Natl. Cancer Inst.* **103**, 1656. https://doi.org/10.1093/jnci/djr393 (2011).
18. Sava, A. et al. Brain metastases originating in breast cancer: Clinical-pathological analysis and immunohistochemical profile. *Roman. J. Morphol. Embryol.* **62**, 435. https://doi.org/10.47162/RJME.62.2.09 (2021).
19. Wang, Y., Ye, F., Liang, Y. & Yang, Q. Breast cancer brain metastasis: Insight into molecular mechanisms and therapeutic strategies. *Br. J. Cancer* **125**, 1056. https://doi.org/10.1038/s41416-021-01424-8 (2021).
20. Gödecke, N., Hauser, H. & Wirth, D. Stable expression by lentiviral transduction of cells. *Methods Mol. Biol.* **2810**, 147–159. https://doi.org/10.1007/978-1-0716-3878-1_10 (2024).
21. Qian, Y. et al. Transduction of lentiviral vectors and ADORA3 in HEK293T cells modulated in gene expression and alternative splicing. *Int. J. Mol. Sci.* **26**(9), 4431. https://doi.org/10.3390/ijms26094431 (2025).

22. Matrai, J., Chuah, M. K. & VandenDriessche, T. Recent advances in lentiviral vector development and applications. *Mol. Ther.* **18**(3), 477–490. https://doi.org/10.1038/mt.2009.281 (2010).
23. Böcker, W. et al. Efficient lentiviral transduction of human mesenchymal stem cells that preserves proliferation and differentiation capabilities. *J. Gene Med.* **9**(7), 585–595. https://doi.org/10.1002/jgm.1049 (2007).
24. Park, J. H. et al. a systems approach to brain tumor treatment. *Cancers* **13**, 3152. https://doi.org/10.3390/cancers13133152 (2021).
25. Rajapakse, V. N., Herrada, S. & Lavi, O. Phenotype stability under dynamic brain-tumor environment stimuli maps glioblastoma progression in patients. *Sci. Adv.* **6**, eaaz4125. https://doi.org/10.1126/sciadv.aaz4125 (2020).
26. Riggio, A. I., Varley, K. E. & Welm, A. L. The lingering mysteries of metastatic recurrence in breast cancer. *Br. J. Cancer* **124**, 13–26. https://doi.org/10.1038/s41416-020-01161-4 (2021).
27. Fares, J. et al. Molecular principles of metastasis: A hallmark of cancer revisited. *Sig. Transduct. Target Ther* **5**, 1–17. https://doi.org/10.1038/s41392-020-0134-x (2020).
28. Perez-Añorve, I. X. et al. Integrated transcriptome analysis of radioresistant cells revealed genes and pathways predictive of tumor response to radiotherapy and chemotherapy in breast cancer. *Adv. Ther.* **7**, 2300274. https://doi.org/10.1002/adtp.202300274 (2024).
29. Boelens, M. C. et al. Exosome transfer from stromal to breast cancer cells regulates therapy resistance pathways. *Cell* **159**, 499. https://doi.org/10.1016/j.cell.2014.09.051 (2014).
30. Sun, Q. et al. Stem-like breast cancer cells in the activated state resist genetic stress via TGFBI-ZEB1. *npj Breast Cancer* **8**, 1–10. https://doi.org/10.1038/s41523-021-00375-w (2022).
31. Wu, M. et al. Cancer stem cell regulated phenotypic plasticity protects metastasized cancer cells from ferroptosis. *Nat. Commun.* **13**, 1371. https://doi.org/10.1038/s41467-022-29018-9 (2022).
32. Qiu, Y., Yang, L., Liu, H. & Luo, X. Cancer Stem cell-targeted therapeutic approaches for overcoming trastuzumab resistance in HER2-positive breast cancer. *Stem Cells* **39**, 1125–1136. https://doi.org/10.1002/stem.3381 (2021).
33. Swain, S. M., Shastry, M. & Hamilton, E. Targeting HER2-positive breast cancer: Advances and future directions. *Nat. Rev. Drug Discov.* **22**, 101–126. https://doi.org/10.1038/s41573-022-00579-0 (2023).
34. Guo, H. et al. The pivotal role of preclinical animal models in anti-cancer drug discovery and personalized cancer therapy strategies. *Pharmaceuticals* **17**, 1048. https://doi.org/10.3390/ph17081048 (2024).
35. Chu, X., Bleasby, K. & Evers, R. Species differences in drug transporters and implications for translating preclinical findings to humans. *Expert Opin. Drug Metab. Toxicol.* **9**, 237–252. https://doi.org/10.1517/17425255.2013.741589 (2013).
36. Ponnusamy, S. et al. Orally bioavailable androgen receptor degrader, potential next-generation therapeutic for enzalutamide-resistant prostate cancer. *Clin. Cancer Res.* **25**, 6764–6780. https://doi.org/10.1158/1078-0432.CCR-19-1458 (2019).
37. Singh, M. & Johnson, L. Using genetically engineered mouse models of cancer to aid drug development: An industry perspective. *Clin. Cancer Res.* **12**, 5312–5328. https://doi.org/10.1158/1078-0432.CCR-06-0437 (2006).
38. Näf, D. et al. The mouse tumor biology database: A public resource for cancer genetics and pathology of the mouse1. *Can. Res.* **62**, 1235–1240 (2002).
39. Oser, M. G. et al. Genetically-engineered mouse models of small cell lung cancer: The next generation. *Oncogene* **43**, 457–469. https://doi.org/10.1038/s41388-023-02929-7 (2024).
40. Kersten, K., de Visser, K. E., van Miltenburg, M. H. & Jonkers, J. Genetically engineered mouse models in oncology research and cancer medicine. *EMBO Mol. Med.* **9**, 137. https://doi.org/10.15252/emmm.201606857 (2016).
41. Noto, F. K., Towobola, B., Arey, A., et al The SRGTM rat: A novel SCID rat for humanization studies.
42. Maffuid, K. & Cao, Y. Decoding the complexity of immune-cancer cell interactions: Empowering the future of cancer immunotherapy. *Cancers* **15**, 4188. https://doi.org/10.3390/cancers15164188 (2023).
43. Mortaz, E. et al. Cancers related to immunodeficiencies: Update and perspectives. *Front. Immunol.* **7**, 365. https://doi.org/10.3389/fimmu.2016.00365 (2016).
44. Tew, B. Y. & Salhia, B. The establishment and utilization of patient derived xenograft models of central nervous system metastasis. *J. Vis. Exp.* **171**, e62264. https://doi.org/10.3791/62264 (2021).
45. Miarka, L. & Valiente, M. Animal models of brain metastasis. *Neurooncol. Adv.* **3**(1), v144–v156 (2021).

Author contributions

N.F., A.D., M.U. and M.M. contributed to data acquisition and manuscript preparation. H.N. contributed to data analysis and manuscript preparation. Q.Z. performed the histopathology evaluation and contributed to manuscript preparation. M.J.S., F.K.N. and D.B. instructed the SRG rat procurement for surgical intervention. J.A.R., J.J.K. and Y.X. performed BCBM cell engineering and instructed the BLI studies. T.J.S. instructed the rat MRI acquisition. S.S. instructed SRG rat surgical management. M.O.H. created the study design and contributed to data analysis and manuscript preparation. All authors reviewed the manuscript.

Funding

This work was supported by the Cancer Research Society, Canadian Institute for Health Research, London Regional Cancer Program and Mitacs Accelerate International.

Declarations

Competing interests

M.O.H. received a Mitacs Accelerate International fellowship partially funded by Hera Biolabs to support research trainees (N.F., H.N.) in this study. N.F., H.N., A.D., M.U, M.M., Q.Z., J.A.R., J.J.K., Y.X., T.J.S., F.K.N., D.B., M.J.S. and S.S. do not have competing interests.

Ethics approval

This study was approved by the Human Research Ethics Board at Western University and carried out in accordance with the Tri-Council Policy for research involving human subjects. All animal protocols were approved by the Animal Care and Use Committee at Western University and carried out in accordance with the Tri-Council Policy for research involving human subjects and the Canadian Council on Animal Care. This study is reported in accordance with ARRIVE guidelines (https://arriveguidelines.org).

Consent to participate

Human tissue was obtained with informed patient consent for research purposes.

Additional information

Correspondence and requests for materials should be addressed to M.O.H.